

Strange quark chiral phase transition in hot 2+1-flavor magnetized quark matter

Márcio Ferreira,^{1,*} Pedro Costa,^{1,†} and Constança Providência^{1,‡}

¹*Centro de Física Computacional, Department of Physics,
University of Coimbra, P-3004-516 Coimbra, Portugal*

(Dated: May 8, 2018)

Using the Polyakov–Nambu–Jona-Lasinio model the strange quark chiral phase transition and the effect of its current mass on a hot magnetized three flavor quark matter at zero chemical potential is investigated. The impact of the 't Hooft mixing term on the restoration of the chiral symmetry on the light and strange sectors is studied and the critical temperature dependence on the magnetic field strength of the chiral strange transition is analyzed. It is shown that the s quark is much less sensitive to the magnetic field than the light quarks. Due to the 't Hooft term, it has a strong influence on the light quarks at all temperatures for small magnetic fields and for temperatures close to the transition temperature at zero magnetic field and above for strong magnetic fields. In particular, the large mass of the s quark makes the chiral transition of the light sector smoother and shifted to larger temperatures. A scalar coupling that weakens when the magnetic field increases will originate an inverse magnetic catalysis also in the s quark and smoothen the signature of the crossover on thermodynamical quantities such as the sound velocities or the specific heat.

PACS numbers: 24.10.Jv, 11.10.-z, 25.75.Nq

I. INTRODUCTION

Strangeness is a very important degree of freedom that must be considered when discussing the QCD phase diagram. The up, down and strange quark masses control the amount of explicit chiral symmetry breaking in QCD. However, in the real world, the strange quark is significantly heavier than the nonstrange quarks which makes the physics related with the strange quark very interesting once the SU(3)-flavor symmetry is explicitly broken by its mass. In fact, chiral symmetry is a very important concept in the up/down sector and even, although with larger deviations, when strange quarks are also included [1]: when two massless quarks are considered (and the strange quark mass is taken to be infinite) the chiral phase transition is of second order, but, in a world with three massless quarks, the chiral phase transition is of first order. If the strange quark mass is reduced from infinity to zero, at some point the phase transition must change from second order to first order and there must be a tricritical strange quark mass, m_s^{tric} , where the second order chiral transition ends and the first order region begins [2].

The relevance of strangeness is transversal to all regions across the phase diagram. In the interior of a neutron star (high density and low temperature region) it is expected that strangeness is present either in the form of hyperons, a kaon condensate or a core of deconfined quark matter [3]. The recent measurement of the mass of the two solar mass millisecond pulsars PSR J1614–2230 [4] and PSR J1903+0327 [5] places quite strong constraints on the core composition of neutron stars. The

compatibility of these large masses with the appearance of strangeness has been questioned on the basis of microscopic approaches to the hadronic equation of state [6, 7]. Within a relativistic mean field approach it has been shown that it is still possible to accommodate these large masses even considering the presence of hyperons or kaons (see for instance [8–12]), since there is a large uncertainty on the coupling of hyperons to nucleons. Another possibility is that the interior of the neutron star contains a quark core [13].

In relativistic heavy-ion collisions the strange and multistrange particle production is an important tool to investigate the properties of the hot and dense matter created in the collision, since there is no net strangeness content in the initially colliding nuclei [14]. An enhanced production of strange particles in A–A compared to pp collisions was one of the first signatures proposed for the deconfined quark-gluon plasma [15, 16]. Very recently, the possibility of multiple chemical freeze-outs was suggested, in particular, the strange freeze-out which would indicate a clear separation of pion and kaon chemical freeze-outs [17]. Based on known systematics of hadron cross sections, it was argued that different particles can freeze out of the fireball produced in heavy-ion collisions at different times. Another alternative approach to treat the strange particle freeze-out separately, with the full chemical equilibrium, was presented in [18]: based on the conservation laws, the connection between the freeze-outs of strange and nonstrange hadrons was achieved. Strangeness freeze-out in heavy-ion collisions is also deserving the attention of lattice QCD (LQCD) community. It was found that experimentally unobserved strange hadrons become thermodynamically relevant in the vicinity of the QCD crossover, modifying the yields of the ground state strange hadrons in heavy-ion collisions, which leads to significant reductions in the chemical freeze-out temperature of strange hadrons [19]. How-

* mferreira@teor.fis.uc.pt

† pcosta@teor.fis.uc.pt

‡ cp@teor.fis.uc.pt

ever, the question whether of hadrons of different quark composition freeze out simultaneously or exhibit a flavor hierarchy [20] still has no answer.

Another relevant aspect of strangeness in the phase diagram refers to the determination of the confinement/deconfinement pseudocritical temperature. At finite temperature and zero chemical potential, LQCD results indicate a crossover from the hadronic phase to the quark-gluon plasma for realistic u , d and s quark masses [21] and there are different prescriptions which lead to different pseudocritical temperatures for both, the chiral and the confinement/deconfinement phase transitions. For the deconfinement transition a way to define the pseudocritical point is to use the peak position of the Polyakov loop susceptibility. However, instead of the Polyakov loop, it is also possible to use the strange quark number susceptibility, $\chi_s = \frac{T}{V} \frac{\partial^2 (\ln Z)}{\partial \mu_s^2}$, to define the pseudocritical temperature, being μ_s the chemical potential for strange quarks. As pointed out in [22], χ_s behaves in a similar way to the Polyakov loop: in the Nambu–Jona-Lasinio (NJL) model coupled to the Polyakov loop (PNJL), when the quark mass of the heavy flavor is large enough, the susceptibility χ_s is proportional to the Polyakov loop, which makes this quantity qualified as an order parameter [22]. So, the inflection point of χ_s gives the pseudocritical temperature consistent with the use of the peak position of the Polyakov loop susceptibility. Lattice data from different collaborations show that the two pseudocritical temperatures are close to each other [23, 24], making this behavior a general trend. In the framework of lattice QCD calculations, the strange quark number susceptibility is also a very interesting quantity from the theoretical point of view because it is related to a conserved current, thus no renormalization ambiguities appear, which makes direct comparisons particularly easy [23].

Recent LQCD results also suggest that the deconfinement of strangeness takes place at the chiral crossover region, and for temperatures larger than twice the chiral crossover temperature, the strangeness carrying degrees of freedom inside the quark-gluon plasma can be described by a weakly interacting gas of quarks [25]. Finally, the direct determination of the light and strange quark condensates from full LQCD was performed in [26].

In heavy-ion collisions it is also important to consider the presence of magnetic fields. Although time dependent and short lived [27], the magnetic fields involved can reach intensities of the order $eB = 5 - 30 m_\pi^2$ (corresponding to $1.7 \times 10^{19} - 10^{20}$ gauss) and temperatures varying from $T = 120 - 200$ MeV. For example, the estimated value of the magnetic field strength for the LHC energy is of the order $eB \sim 15 m_\pi^2$ [28].

At zero chemical potential and finite temperature, when the effect of an external magnetic field in QCD matter with $N_f = 2 + 1$ flavors with physical quark masses is taken into account, LQCD results show that light and heavy quark sectors respond differently to the magnetic field [29]. The magnetic field suppresses the

light quark condensates near the transition temperature, giving them a nonmonotonic behavior with eB . However, according to [30], the s quark condensate increases with eB for all temperatures. Furthermore, it was observed in [29] that the pseudocritical temperatures for $N_f = 3$ heavy flavors do not change much with the magnetic field. The Polyakov loop also reacts to the magnetic field: it increases sharply with the magnetic field around the transition temperature and the transition temperature taken from the renormalized Polyakov loop clearly decreases with the magnetic field [31].

Low-energy effective models, namely the NJL and PNJL in 2+1 flavors, have also been used to study the influence of an external magnetic field in the QCD phase diagram at zero chemical potential and finite temperature [32–34]. At finite temperature and chemical potential the combined effects of the strangeness, isospin asymmetry and an external magnetic field on the location of the critical end point (CEP) in the QCD phase diagram were investigated [35]. It was shown that isospin asymmetry shifts the CEP to larger baryonic chemical potentials and smaller temperatures, and that at large asymmetries the CEP disappears. However, a strong enough magnetic field drives the system into a first order phase transition. It was also discussed that strangeness shifts the CEP to larger baryonic densities and in most cases also to larger baryonic chemical potentials.

Almost all low-energy effective models, at zero chemical potential, including the NJL-type models, find an enhancement of the condensate due to the magnetic field, the so-called magnetic catalysis, and no reduction of the pseudocritical chiral transition temperature with the magnetic field [36–38]. However, recent studies using the NJL and PNJL [39] could reproduce the inverse magnetic catalysis (IMC) effect predicted by LQCD, if a magnetic field dependent scalar coupling that decreases when the field increases is considered. This dependence of the coupling allows us to reproduce the LQCD results with respect to the quark condensates and to the Polyakov loop: due to the magnetic field the quark condensates are enhanced at low and high temperatures and suppressed for temperatures close to the transition temperature [29, 30].

In this paper we will investigate the strange quark chiral phase transition in a hot 2+1-flavor magnetized quark matter and identify the features of the QCD phase diagram due to the presence of strangeness. The main property that distinguishes the u and d quarks from the s quark is its mass, more than one order of magnitude larger. Moreover, a term like the 't Hooft term, that mixes flavors, will have a significant effect, and the behavior of the u and d quarks will be strongly influenced by the s quark. We will analyze how these features affect the QCD phase diagram and will identify the importance of including the strangeness degree of freedom.

II. MODEL AND FORMALISM

A. Model Lagrangian and gap equations

We describe three flavor ($N_c = 3$) quark matter subject to strong magnetic fields within the 2+1 PNJL model. The PNJL Lagrangian with explicit chiral symmetry breaking, where the quarks couple to a (spatially constant) temporal background gauge field, represented in terms of the Polyakov loop, and in the presence of an external magnetic field is given by [40]:

$$\mathcal{L} = \bar{q} [i\gamma_\mu D^\mu - \hat{m}_f] q + \mathcal{L}_{sym} + \mathcal{L}_{det} + \mathcal{U}(\Phi, \bar{\Phi}; T) - \frac{1}{4} F_{\mu\nu} F^{\mu\nu}, \quad (1)$$

where the quark sector is described by the SU(3) version of the NJL model which includes scalar-pseudoscalar and the 't Hooft six fermion interactions, that models the axial $U_A(1)$ symmetry breaking [41], with \mathcal{L}_{sym} and \mathcal{L}_{det} given by [1]

$$\mathcal{L}_{sym} = G_s \sum_{a=0}^8 [(\bar{q}\lambda_a q)^2 + (\bar{q}i\gamma_5\lambda_a q)^2], \quad (2)$$

$$\mathcal{L}_{det} = -K \{ \det [\bar{q}(1 + \gamma_5)q] + \det [\bar{q}(1 - \gamma_5)q] \} \quad (3)$$

where $q = (u, d, s)^T$ represents a quark field with three flavors, $\hat{m}_f = \text{diag}_f(m_u, m_d, m_s)$ is the corresponding (current) mass matrix, $\lambda_0 = \sqrt{2/3}I$ where I is the unit matrix in the three flavor space and $0 < \lambda_a \leq 8$ denote the Gell-Mann matrices. The coupling between the (electro)magnetic field B and quarks, and between the effective gluon field and quarks, is implemented *via* the covariant derivative $D^\mu = \partial^\mu - iq_f A_{EM}^\mu - iA^\mu$ where q_f represents the quark electric charge ($q_d = q_s = -q_u/2 = -e/3$), A_μ^{EM} and $F_{\mu\nu} = \partial_\mu A_\nu^{EM} - \partial_\nu A_\mu^{EM}$ are used to account for the external magnetic field and $A^\mu(x) = g_{strong} \mathcal{A}_a^\mu(x) \frac{\lambda_a}{2}$ where \mathcal{A}_a^μ is the SU_c(3) gauge field. We consider a static and constant magnetic field in the z direction, $A_\mu^{EM} = \delta_{\mu 2} x_1 B$. In the Polyakov gauge and at finite temperature the spatial components of the gluon field are neglected: $A^\mu = \delta_0^\mu A^0 = -i\delta_4^\mu A^4$. The trace of the Polyakov line defined by $\Phi = \frac{1}{N_c} \langle \langle \mathcal{P} \exp i \int_0^\beta d\tau A_4(\vec{x}, \tau) \rangle \rangle_\beta$ is the Polyakov loop which is the *exact* order parameter of the \mathbb{Z}_3 symmetric/broken phase transition in pure gauge.

The coupling constant G_s in \mathcal{L}_{sym} denotes the scalar-type four-quark interaction of the NJL sector. Since the model is not renormalizable, we use as a regularization scheme a sharp cutoff in three-momentum space, Λ , only for the divergent ultraviolet integrals (the details can be found in Ref. [42]). The parameters of the model, Λ , the coupling constants G_s and K and the current quark masses m_u , m_d and m_s are determined by fitting f_π , m_π , m_K , and $m_{\eta'}$ to their empirical values. We consider $\Lambda = 602.3 \text{ MeV}$, $m_u = m_d = 5.5 \text{ MeV}$, $m_s = 140.7 \text{ MeV}$, $G\Lambda^2 = 1.385$ and $K\Lambda^5 = 12.36$ as in [43].

To describe the pure gauge sector an effective potential $\mathcal{U}(\Phi, \bar{\Phi}; T)$ is chosen in order to reproduce the results obtained in lattice calculations [44]:

$$\frac{\mathcal{U}(\Phi, \bar{\Phi}; T)}{T^4} = -\frac{a(T)}{2} \bar{\Phi} \Phi + b(T) \ln [1 - 6\bar{\Phi} \Phi + 4(\bar{\Phi}^3 + \Phi^3) - 3(\bar{\Phi} \Phi)^2], \quad (4)$$

where $a(T) = a_0 + a_1 \left(\frac{T_0}{T}\right) + a_2 \left(\frac{T_0}{T}\right)^2$, $b(T) = b_3 \left(\frac{T_0}{T}\right)^3$. The standard choice of the parameters for the effective potential \mathcal{U} is $a_0 = 3.51$, $a_1 = -2.47$, $a_2 = 15.2$, and $b_3 = -1.75$.

As is well known, the effective potential exhibits the feature of a phase transition from color confinement ($T < T_0$, the minimum of the effective potential being at $\Phi = 0$) to color deconfinement ($T > T_0$, the minimum of the effective potential occurring at $\Phi \neq 0$).

We know that the parameter T_0 of the Polyakov potential defines the onset of deconfinement and is normally fixed to 270 MeV according to the critical temperature for the deconfinement in pure gauge lattice findings (in the absence of dynamical fermions) [45]. When quarks are added to the system, quark backreactions must be taken into account, thus a decrease in T_0 to 210 MeV is required to obtain the deconfinement pseudocritical temperature given by LQCD, within the PNJL model. Therefore, the value of T_0 is fixed in order to reproduce LQCD results ($\sim 170 \text{ MeV}$ [46]).

The thermodynamical potential for the three flavor quark sector Ω is written as

$$\Omega(T, \mu) = G_s \sum_{i=u,d,s} \langle \bar{q}_i q_i \rangle^2 + 4K \langle \bar{q}_u q_u \rangle \langle \bar{q}_d q_d \rangle \langle \bar{q}_s q_s \rangle + \mathcal{U}(\Phi, \bar{\Phi}, T) + \sum_{i=u,d,s} (\Omega_{vac}^i + \Omega_{med}^i + \Omega_{mag}^i) \quad (5)$$

with the flavor contributions from vacuum Ω_{vac}^i , medium Ω_{med}^i and magnetic field Ω_{mag}^i [42].

III. RESULTS

In the present section we investigate the effect of the magnetic field on the strange quark chiral phase transition. The strange quark is strongly coupled to the light quarks through the 't Hooft term. It has already been shown that a $U_A(1)$ anomaly reduction in the medium has the effect of weakening the chiral phase transition [47]. Therefore, understanding the strange quark chiral phase transition requires that the effect of the 't Hooft term is understood. Another aspect already mentioned is its high mass when compared with the light quarks. In order to feel an effect similar to the d quark in the presence of a magnetic field, a much stronger field must be applied.

In the following we analyze the effect of the 't Hooft term, the current s quark mass and the inverse magnetic

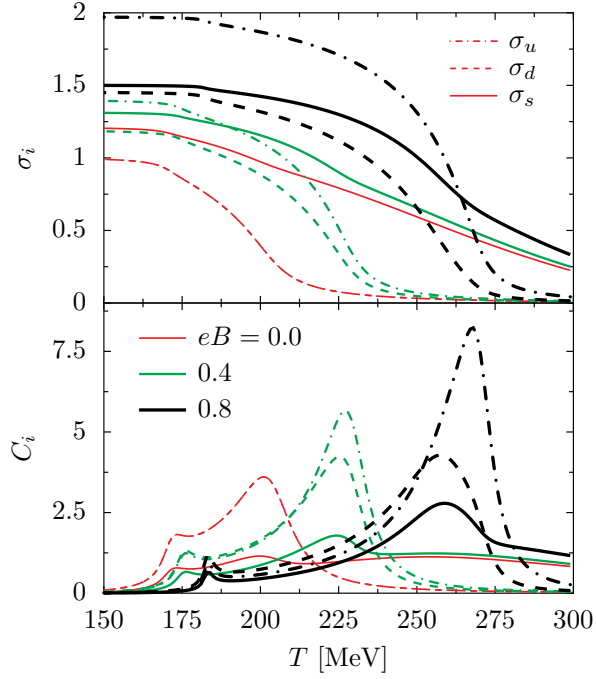


FIG. 1. The quark condensates and their susceptibilities as a function of temperature for three magnetic field strengths: $eB = 0.0, 0.4$ and 0.8 GeV^2 .

catalysis effect that can be taken into account by setting a magnetic field dependent scalar coupling [39].

We first analyze the order parameters within the complete PNJL model, including the 't Hooft term. In Fig. 1 the normalized quark condensates $\sigma_i = \langle \bar{q}_i q_i \rangle(B, T) / \langle \bar{q}_i q_i \rangle(0, 0)$ and their respective susceptibilities $C_i = -m_\pi \partial \sigma_i / \partial T$ are plotted for three magnetic field strengths. The quark condensates are normalized by the up quark vacuum condensate value at zero magnetic field, and the inclusion of the pion mass m_π in the susceptibilities assures a dimensionless quantity. The quark condensates are enhanced by the presence of the magnetic field, effect known by magnetic catalysis. For $eB = 0.8 \text{ GeV}^2$, due to the quark electric charge difference, the condensate σ_u is larger than σ_s , even though the current strange quark current mass m_s is larger than the current u quark mass m_u . The first peaks in the susceptibilities at low temperatures are induced by the deconfinement transition, i.e. by the rapid change of the Polyakov loop with temperature, that signals the deconfinement phase transition. As already pointed out in [32], compared with the chiral transition, the deconfinement phase transition is quite insensitive to the presence of the magnetic field.

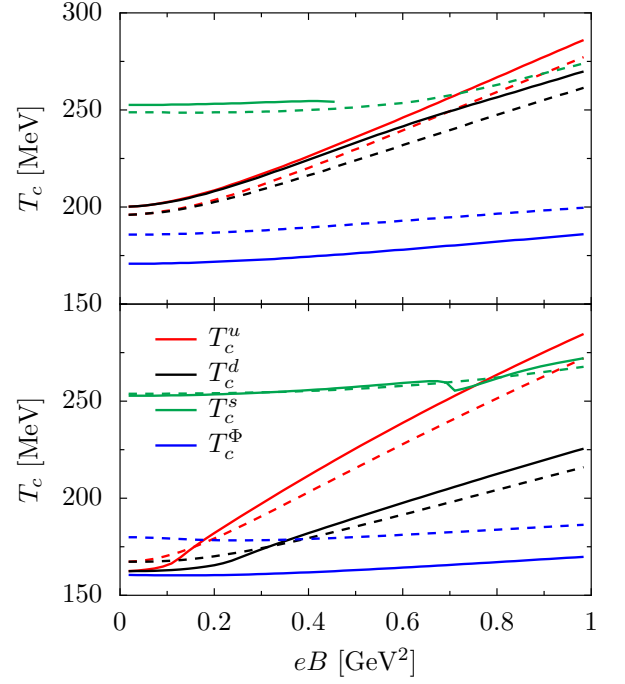


FIG. 2. The critical temperatures (T_c^i) as a function of eB , for $K \neq 0$ (top panel) and $K = 0$ (bottom panel), using the peak of the susceptibilities (solid lines) and half the vacuum value of the order parameters (dashed lines).

A. The impact of the 't Hooft term on the chiral phase transitions

In order to analyze the impact of the 't Hooft term on the transition temperatures of the chiral transition as a function of the magnetic field strength, we calculate the transition temperatures with $K \neq 0$ and $K = 0$. The results are shown in Fig. 2. Two criteria are used to calculate the transition temperatures: (i) the peaks of the respective susceptibilities and (ii) the temperature T_c^i at which the order parameter is half the respective vacuum value, $\langle \bar{q}_i q_i \rangle(B, T_c^i) = 0.5 \langle \bar{q}_i q_i \rangle(B, 0)$. For the $K \neq 0$ case (top panel), using the first criteria (solid lines), the critical temperature for the strange quark can only be calculated up to some maximum eB value. For higher eB values, the chiral transition for the u and d quarks washes out the strange quark transition and the inflection point of the strange quark condensate, which defines the strange quark phase transition, cannot be defined anymore. This can be solved if the second criterion (dashed lines) is used. With the second criteria, a similar behavior is obtained for the s quark, but with lower transition temperatures. From the top panel of Fig. 2 it is also seen that the transition temperatures for the light quarks increase faster with eB than for the s quark. In fact, the strange transition temperature is almost insensitive to the magnetic field strength up to $eB \approx 0.4 \text{ GeV}^2$, mainly due to its larger mass. Another interesting aspect that can be seen is the increase of the splitting be-

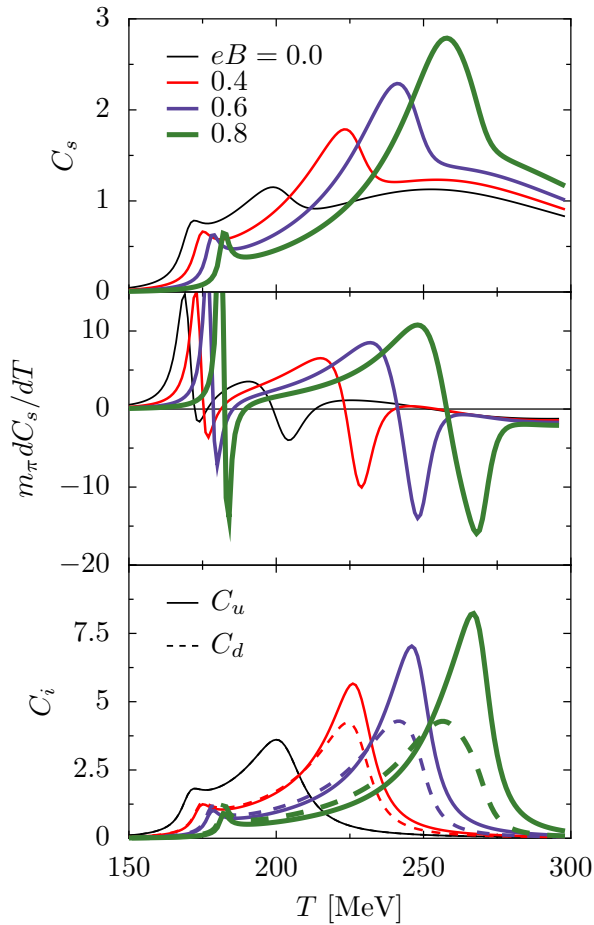


FIG. 3. (Top panel) The strange quark susceptibilities C_s , (middle panel) dC_s/dT and (bottom panel) the u (solid lines) and d (dashed lines) quark susceptibilities $C_{u,d}$ as a function of eB with the 't Hooft term.

tween the temperatures at which chiral transitions occur, for the light quarks, and the deconfinement temperature. This particular feature was already found in the context of the linear sigma model coupled to quarks and to the Polyakov loop in [48]. The Sakai-Sugimoto model also predicts a similar behavior [49].

Comparing the $K = 0$, Fig. 2 bottom panel, with the $K \neq 0$ case, Fig. 2 top panel, some important features should be pointed out in the light quark sector: (1) for low eB values, smaller chiral transition temperatures are obtained, and the difference $T_c^u - T_c^d$ increases faster with eB ; (2) for low eB values, and using the second criterion for the transition temperature, the deconfinement transition temperature lies above the chiral transitions temperatures as obtained in LQCD calculations; (3) at $eB \approx 0$, the gap between the chiral and deconfinement transitions is quite small. We conclude that the quark chiral transitions and the deconfinement transition are strongly correlated due to the 't Hooft term, and some features of the QCD phase diagram are precisely defined by this term.

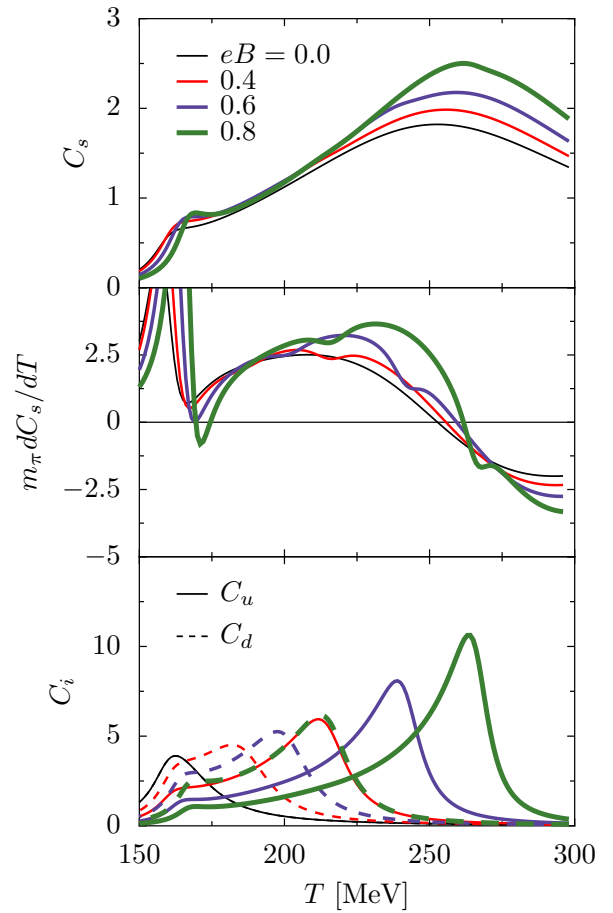


FIG. 4. (Top panel) The strange quark susceptibilities C_s , (middle panel) dC_s/dT and (bottom panel) the u (solid lines) and d (dashed lines) quark susceptibilities $C_{u,d}$ as a function of eB without the 't Hooft term.

In order to understand how the magnetic fields affect the strange quark and, thus, its critical temperature, it is important to determine the impact that the chiral restoration of the light sector has on the behavior of the strange quark condensate. In Figs. 3 and 4 we calculate for $K \neq 0$ and $K = 0$, respectively, the strange quark susceptibilities C_s (top panel), the derivative of the susceptibilities $m_\pi dC_s/dT$ (middle panel), and the susceptibilities of the light quarks $C_{u,d}$ (bottom panel), for several values of eB . For $K \neq 0$, the strange quark transition is influenced more strongly by the chiral restoration of the light sector than for $K = 0$. In fact, with $K \neq 0$, the most pronounced peak in the strange quark susceptibility C_s is due to the chiral transition of the u and d quarks (see Fig. 3 bottom panel), because with a finite 't Hooft term the gap equations mix all flavors.

The strange quark transition is reflected in the last inflection point of C_s . In the middle panel of Fig. 3, it is seen that for $eB = 0.6 \text{ GeV}^2$ this inflection point disappears, being washed out by the transition of the light quarks. With $K = 0$ there is no flavor mixing in the gap equations, and the strange quark phase transition

is clearly identified in the susceptibility. Although some bumps still appear in the derivative of the C_s due to the light quarks, their intensity is much weaker than the transition of the strange quark itself. The mixing occurs through the distribution functions. The no flavor mixing for $K = 0$ is confirmed in the bottom panel of Fig. 4, where it is seen that there is no direct coupling between the u and d quarks as the magnetic field increases.

B. The impact of the current strange quark mass on its transition temperature

As we have seen in the last section, the restoration of the chiral symmetry of the strange quark has a different behavior when compared with the light quarks due to its larger current mass: $m_s \approx 25.5m_{u,d}$. For low magnetic field strengths, the critical temperature of the strange quark does not change much as compared with the light quarks. As expected, the restoration of the chiral symmetry will depend not only on the quark electric charges but also on their current quark masses. Effects of the magnetic field become noticeable when eB becomes of the order of the quark mass squared.

Next we will analyze how the restoration of the chiral symmetry depends on the value of the strange quark current mass m_s , keeping $m_{u,d} = 5.5$ MeV. In this section the PNJL model with 't Hooft term ($K = 12.36/\Lambda^5$) will be used. In NJL and PNJL models, at $eB = 0$, this dependence was investigated in [50].

We first investigate the impact of the current mass of the strange quark on the quark condensates. In Fig. 5 the renormalized quark condensates are plotted as function of temperature, for $eB = 0.1$ GeV² (top panel) and $eB = 0.5$ GeV² (bottom panel), using three values of strange current mass: $m_s = m_{u,d} = 5.5$ MeV, 40 MeV, and 140.7 MeV. We have renormalized the condensates as $\sigma_i(B, T) = \sigma_i(B, T)/\sigma_u(0, 0)$, where $\sigma_u(0, 0)$ is the vacuum condensate at zero magnetic field, with the current mass of the u quark. For $m_s = m_{u,d}$, the three quarks form an isospin triplet that is broken by the magnetic field presence. Therefore, the differences in the condensates are only induced by the electric charge of each quark, having the σ_u as the highest value ($|q_u| = 2e/3$), and both σ_d and σ_s the lowest ($|q_{d,s}| = e/3$). The effect of the charge is always present independently of the quark masses.

The degeneracy of both σ_d and σ_s is lifted when we set $m_{u,d} \neq m_s$, that is, for $m_s = 40$ and 140.7 MeV. We see that for a low magnetic field strength, 0.1 GeV² (Fig. 5 top panel), for $m_s = m_{u,d}$ (red), the u condensate due to its electric charge has the highest value at any temperature. However, if $m_s = 40$ (black line) and 140.7 MeV (green line), the s quark condensate has the highest value. At low eB the magnetic catalysis effect is mainly determined by the charge of the quark if m_s is of the order of $m_{u,d}$, but this effect becomes weaker with increasing mass m_s . As the strange current quark mass increases

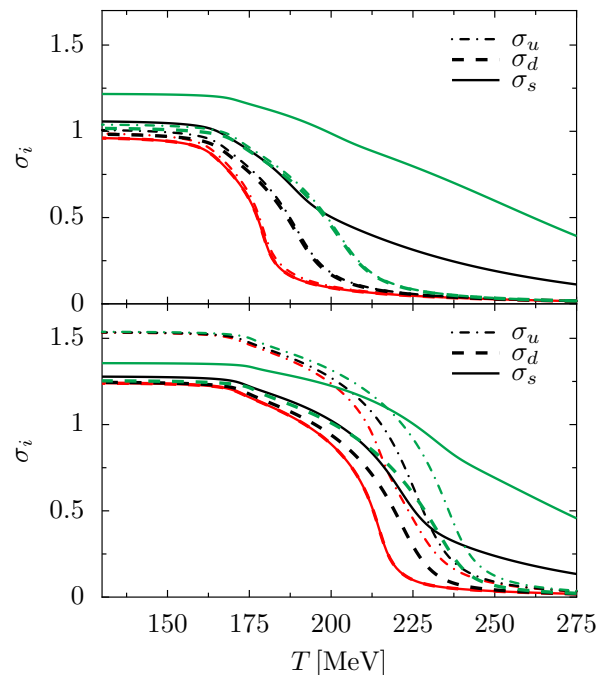


FIG. 5. The order parameters as a function of temperature for $m_s = m_{u,d} = 5.5$ MeV (red lines), $m_s = 40$ MeV (black lines), and $m_s = 140.7$ MeV (green lines) for $eB = 0.1$ GeV² (top panel) and 0.5 GeV² (bottom panel).

the restoration of chiral symmetry in the light sector is pushed to higher temperatures, due to the flavor mixing induced by the 't Hooft term.

For larger magnetic fields, i.e. 0.5 GeV² (Fig. 5 bottom panel) and at low temperatures, the u and d quark condensates are not much affected by the m_s value. The effect of the quark electric charge in the magnetic catalysis at low temperatures predominates over the effect of the strange current quark mass.

In Fig. 6, we fix the m_s value to its current mass of 140.7 MeV, and calculate the quark condensates (top panel) and masses (bottom panel) as a function of eB , for three temperature values. The different behavior between both sectors is clear: for $T = 240$ and 270 MeV, and at low eB , the light quarks are in a restored chiral phase, but at some higher value of eB , the magnetic field drives the light quarks into a chiral broken phase, manifested in the sudden increase of the condensate values. This occurs at larger values of eB for larger temperatures. The values of the strange quark condensate and mass are high for all the magnetic field intensity range shown, and for the three temperatures. Although it is difficult to define the chiral restored/broken phase for the strange quark, we can see a similar behavior as in the light sector, mainly from the bottom panel with the quark masses at $T = 240$ and 270 MeV: the strange quark condensate increases slightly with eB for low magnetic fields and at some value of eB there is a steeper increase of the masses.

In Fig. 7 we perform the same calculation as we did in

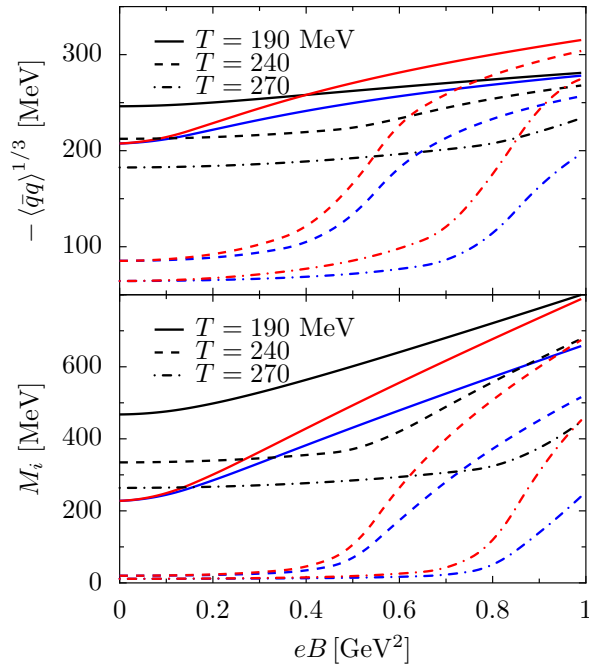


FIG. 6. The condensates (top panel) and masses (bottom panel) of the s (black lines), u (red lines), and d (blue) quarks as a function of eB for several temperatures ($m_s = 140.7$ MeV).

Fig. 6, but now for three m_s values: 5.5 MeV, 40 MeV, and 140.7 MeV. In the bottom panel we have three degenerate quark masses and, as said before, the differences between the different flavors are only due to the quark electric charge. As m_s increases, in the center and top of Fig. 7 (left), the strange quark condensate gets less affected by eB , reflecting its higher constituent mass and the consequent shift of the chiral restoration to larger temperatures. As can be seen on the right panel of Fig. 7, the light sector also feels the change in m_s . This is more clearly seen for $T = 190$ MeV: in this case the condensates soften with increasing m_s . As m_s increases its value, due to the flavor mixing, not only the critical transition temperature of the strange quark increases, but also the transition of the light quarks is shifted to larger temperatures.

We will next calculate the critical temperatures as a function of eB for two cases: an intermediate case between the light and heavy quark sectors, $m_s = 40$ MeV, and an extreme heavy case, $m_s = 300$ MeV. The result is presented in Fig. 8. Two main conclusions can be drawn: (1) for $m_s = 40$ MeV and at high magnetic fields ($eB > 0.3$ GeV²), the transition of the strange quark occurs at the same temperature as the d quark. This indicates that at sufficiently high magnetic field, the critical temperatures at which the chiral symmetry restoration occurs are mainly determined by the electric charge of the quark, because the current quark masses of all quarks are not too different; (2) for $m_s = 300$ MeV, the critical temperature of the strange quark does not change much

with the magnetic field due to its very large mass.

Although the magnetic catalysis affects all quarks, the light sector shows an increase of the critical temperature with the magnetic field while the strange sector is almost insensitive at low magnetic fields, and increases slightly for high magnetic fields.

C. Inverse magnetic catalysis

LQCD results show that the chiral and the deconfinement transition decreases with the magnetic field [29]. This is due to the inverse magnetic catalysis mechanism, which suppresses the condensates near the crossover transition and favors higher values for the Polyakov loop. Within effective models, and, in particular, in the PNJL model, there have been several attempts to reproduce the inverse magnetic catalysis mechanism [32, 39, 51]. In [39], a magnetic field dependent coupling $G_s(eB)$ was introduced: this dependence was fitted to reproduce, within the NJL model, the renormalized critical temperature of the chiral transition given by LQCD [29]. Therefore, it is interesting to study the strange quark transition using this approach. We take $G_s(eB)$ as defined in [39]

$$G_s(\zeta) = G_s^0 \left(\frac{1 + a\zeta^2 + b\zeta^3}{1 + c\zeta^2 + d\zeta^4} \right) \quad (6)$$

where $a = 0.0108805$, $b = -1.0133 \times 10^{-4}$, $c = 0.02228$, $d = 1.84558 \times 10^{-4}$ and $\zeta = eB/\Lambda_{QCD}^2$ with $\Lambda_{QCD} = 300$ MeV.

We have plotted in Fig. 9 the quark condensates and the susceptibilities using $G_s(eB)$. In Fig. 10 the critical temperatures are plotted as a function of eB . All critical temperatures decrease with eB . Looking at the condensates behavior, we see that all of them are enhanced at low temperatures, suppressed at temperatures near the transition temperature and enhanced again at high temperatures. Also the first peaks in the susceptibilities, induced by the deconfinement transition, are shifted to lower temperatures with increasing eB . A larger m_s would still give rise to the same kind of effects but less pronounced.

In order to understand why the critical temperature of the strange quark can only be defined up to a certain eB (using the first criteria), we show in the lower panel of Fig. 9 a zoom of the strange transition region. The maximum of the strange susceptibility induced by the chiral transition of the strange quark is washed out for larger eB values.

The IMC effect is strongly influenced by the 't Hooft term as we will show in the following. In Fig. 11 the u , d and s condensates normalized to their values for a zero magnetic field are plotted for a magnetic field dependent coupling $G_s(eB)$ and different scenarios for the 't Hooft term: with the 't Hooft term (upper panel); with the 't Hooft term switched off, but no refitting of the couplings in order to reproduce the vacuum properties of the pion

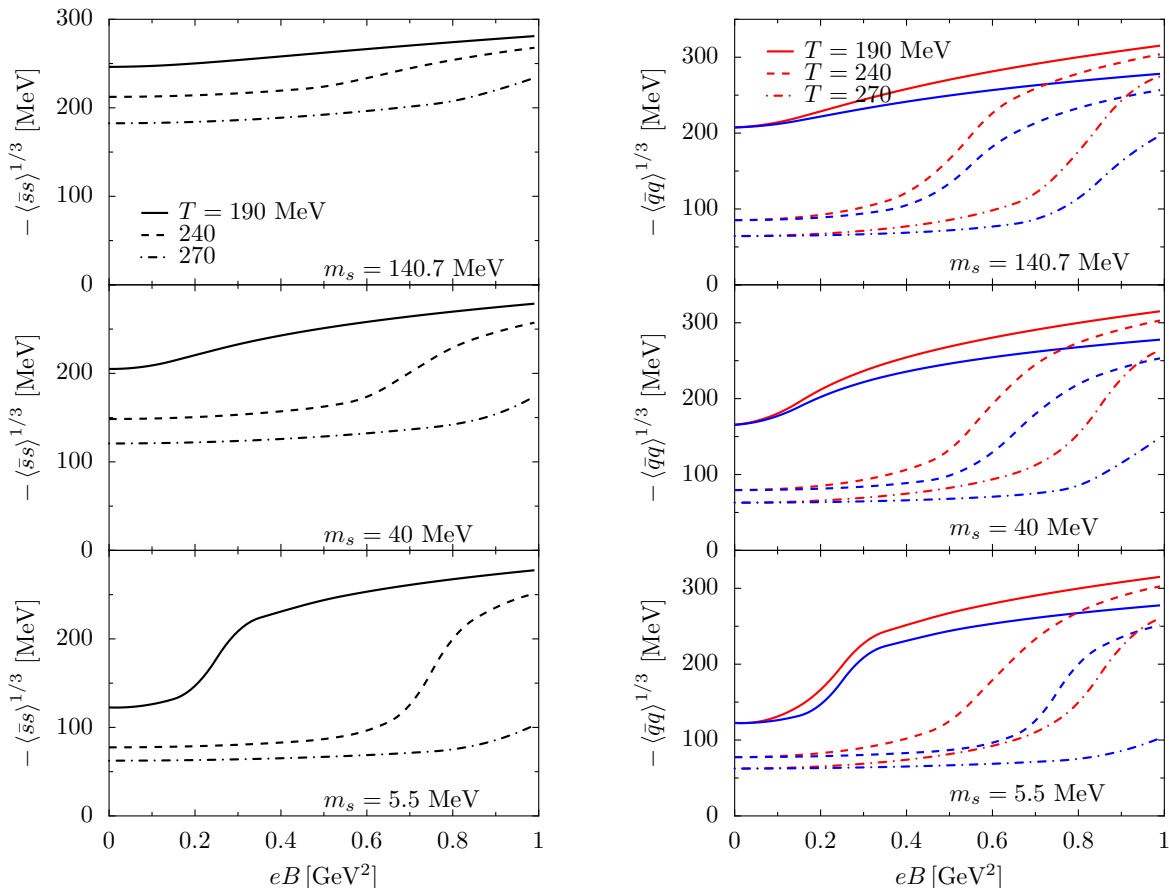


FIG. 7. The quark condensates: s (left), u (red lines) and d (blue lines) (right panel) for several temperatures for three current strange quark mass values: 140.7 MeV (top panels), 40 MeV (middle panels), and 5.5 MeV (bottom panels).

and kaon (middle panel); we switch off the 't Hooft term and use the parametrization proposed in [52] that reproduces the pion and kaon properties without the 't Hooft term (bottom panel).

Just like the u and d quarks, the s quark also shows the inverse magnetic catalysis effect: see in Fig. 11 (upper panel) the dashed-dotted lines. The strange quark condensate presents a nonmonotonic behavior as a function of eB , and its critical temperature is a decreasing function of eB . This behavior is not following the trend indicated in [30], where the s quark condensate is said to increase with growing B for all temperatures. The IMC effect is still present if the K is set to zero: see Fig. 11 (middle panel). In this case the d and s quarks fill a stronger IMC effect, because the mixing with the u quark, with a much larger magnetic catalysis effect due to its larger charge, which prevents a fast decrease of the other condensates, does not exist. The results of Fig. 11 (bottom panel) were also obtained excluding the 't Hooft term, but using a different parametrization that describes the vacuum properties of the pion and kaon [52]. The general behavior is similar to the results shown in the middle panel, although the u quark shows a behavior closer to the upper panel, were the 't Hooft term was

included. This is due to the larger mass of the u quark within parametrization [52], that compensates the effect of the strong magnetic field due to its higher charge.

It is worth pointing out that the behavior of the s quark condensate is expectable. Being the quark with larger mass, it will not feel a strong magnetic catalysis for weak fields. Moreover, its charge is half of the u quark charge, and, therefore, it is also not as affected as the u quark. On the other hand, the IMC effect is implemented in the present model through a parametrization of the scalar coupling, and, consequently, is switched on as soon as $eB > 0$. From these two effects, it results that the s quark also feels the IMC effect. This is clearly seen by switching off the 't Hooft term. In this case no mixing with the u quark occurs and the s condensate decreases for low eB even for $T = 0$.

D. Thermodynamical properties

In the following we will discuss several thermodynamical quantities that allow us to study some observables that are accessible in lattice QCD at zero chemical potential. For example, full results on the QCD equa-

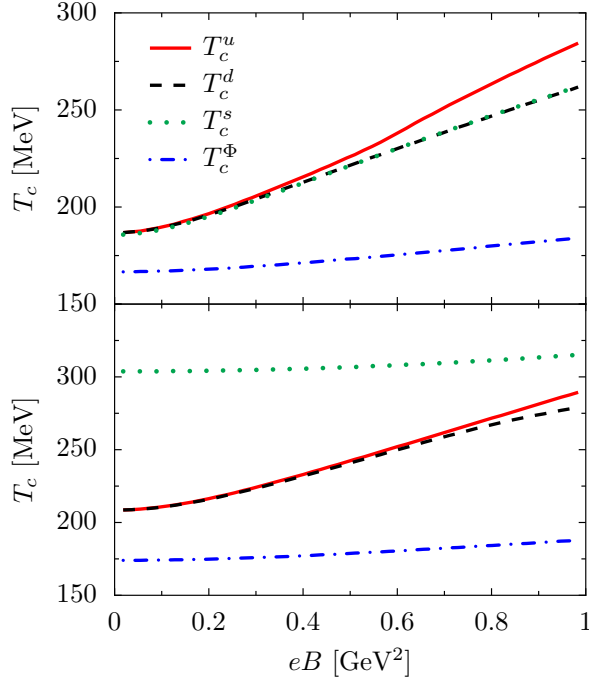


FIG. 8. The critical temperatures for two values of the current quark mass as a function of eB : $m_s = 40$ MeV (top panel) and $m_s = 300$ MeV (bottom panel).

tion of state with 2+1 flavors at zero magnetic field were obtained in [53] and, very recently, LQCD results also in 2+1 flavors with physical quark masses and at nonzero magnetic fields were reported in [54]. By using the hadron resonance gas model the QCD equation of state at nonzero magnetic fields had already been performed in [55]. Here we calculate the following: the pressure $P(T, B) = -[\Omega(T, B) - \Omega(0, B)]$, the energy density $\mathcal{E} = TS - P$ where S is the entropy density, the interaction measure $\Delta = (\mathcal{E} - 3P)/T^4$ that quantifies the deviation from the equation of state of an ideal gas of massless constituents, the speed of sound squared

$$v_s^2 = \left(\frac{\partial P}{\partial \mathcal{E}} \right)_V, \quad (7)$$

and the specific heat

$$C_V = \left(\frac{\partial \mathcal{E}}{\partial T} \right)_V. \quad (8)$$

LQCD studies show that the interaction measure remains large even at very high temperatures, where the Stefan-Boltzmann limit is not yet reached, and thus some interaction must still be present.

In Fig. 12 we have plotted these quantities including the 't Hooft term and a constant scalar coupling G_s^0 (left panel) or a magnetic field dependent scalar coupling $G_s(eB)$ (middle panel), and excluding the 't Hooft term (right panel), for a magnetic field $eB = 0.3$ GeV² (the order of the maximal magnetic field strength for the LHC [28]).

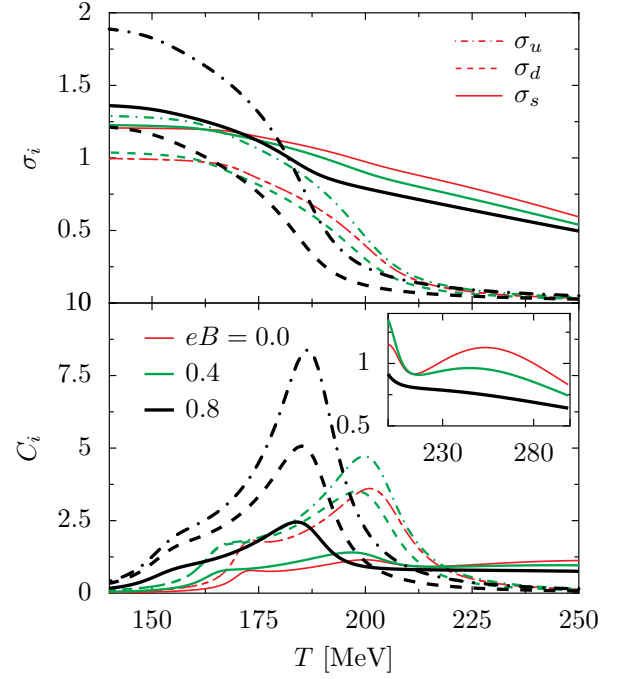


FIG. 9. The quark condensates and their susceptibilities as a function of temperature for $eB = 0.0, 0.4$ and 0.8 GeV², using $G_s(eB)$.

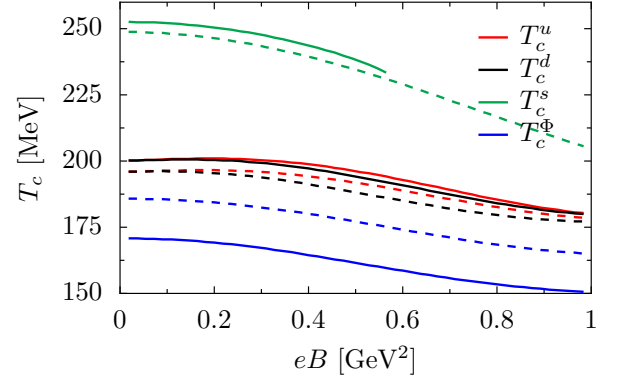


FIG. 10. The critical temperatures T_c^i as a function of eB , given by the peak of the susceptibilities (solid lines) and half the vacuum value of the order parameters (dashed lines), using $G_s(eB)$.

Vertical lines have been included in all panels to indicate the position of the maximum of the quark susceptibilities. In the middle panel the vertical lines are located at the same temperatures of the left panel to show how the magnetic field dependence of the coupling affects the position of the specific heat maximum.

As discussed before, the 't Hooft term pushes the deconfinement and chiral transition temperatures to larger temperatures. Moreover, for the magnetic field shown the u and d quark susceptibility maximum coincide approximately including the 't Hooft term but occur at quite different temperatures for $K = 0$ (Fig. 12 right panel).

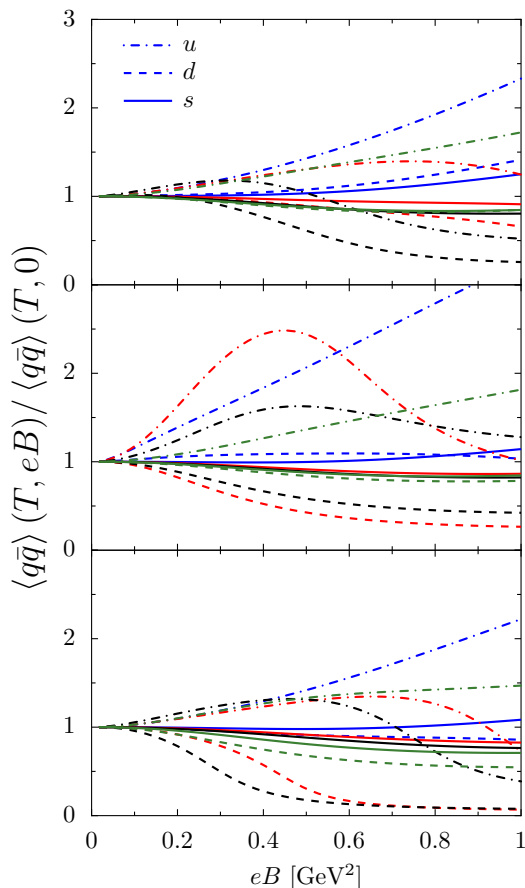


FIG. 11. The ratios of the u , d and s condensates, $\langle q_i \bar{q}_i \rangle(T, eB) / \langle q_i \bar{q}_i \rangle(T, 0)$, as a function of eB , for several values of T [0 (blue lines), 180 (red lines), 200 (black lines) and 250 (green lines) MeV] using $G_s(eB)$: upper panel including the 't Hooft term; middle panel excluding the 't Hooft term without refitting the other parameters; and bottom panel excluding the 't Hooft term and using the parametrization of Ref. [52].

This correlation between the u and d quarks will only be destroyed for much stronger magnetic fields as seen in Fig. 2.

For the three different scenarios considered it is seen that the pressure, the energy density and thus the interaction measure are continuous functions of the temperature as expected if we are in the presence of a crossover. There is a sharp increase in the vicinity of the transition temperature and then a tendency to saturate at the corresponding ideal gas limit. Excluding the 't Hooft term makes all curves smoother. The sharp increase occurs at lower temperatures if a magnetic field dependent coupling $G_s(eB)$ is considered because the transition temperatures are pushed to lower temperatures because the interaction is weakened.

The middle panels of Fig. 12 show the scaled specific heat C_V/T^3 and the speed of sound squared v_s^2 as a function of the temperature. The specific heat presents two peaks, caused by the distinct deconfinement and chiral

transitions. Again, the effect of the magnetic field dependent scalar coupling that pushes the peaks to lower temperatures is clearly seen. Moreover, there is a larger superposition between the Polyakov loop and u and d quark susceptibilities and less pronounced peaks are observed. The second peak corresponding to the chiral transition is almost washed out when no 't Hooft term is included, due to the large superposition of the Polyakov loop and quark susceptibilities.

The speed of sound squared v_s^2 passes through a local minimum around the deconfinement temperature and reaches the limit of $1/3$ (Stefan-Boltzman limit) at high temperature. The minimum indicates the fast change in the quark masses. A second inflection occurs at the chiral transition. As expected from the previous discussion, both features are more pronounced within the PNJL with 't Hooft term and a constant scalar coupling. A comment that should be made is that, for the magnetic field considered $eB = 0.3 \text{ GeV}^2$, the peak on the s quark susceptibility has no effect on all the quantities represented, showing that the influence of the light quark sector is predominant over the strange quark one because the restoration of the chiral symmetry already happened in the light quark sector.

IV. CONCLUSIONS

In the present work we have studied the effect of the strange quark on the QCD phase diagram using a 2+1 PNJL model. Although under most conditions it is enough to consider the u and d quark degrees of freedom, both in heavy-ion collisions and neutron stars, strangeness plays an important role. It is therefore important to identify the features of the QCD phase diagram due to the presence of strangeness in the presence of a magnetic field.

The main property that distinguishes the u and d quarks from the s quark is its mass, more than one order of magnitude larger. We have analyzed the effect of the current s quark mass on the QCD phase diagram at zero chemical potential by considering several values, from a mass equal to that of the u and d quarks to a mass two times the s quark mass in the vacuum. Within the PNJL the 't Hooft term strongly mixes the flavors and, therefore, even the properties of the u and d quarks are strongly influenced by the s quark. This is easily seen comparing the QCD phase diagram features with and without the 't Hooft term when the flavors are decoupled.

We have shown that if the mass of the s quark was closer to the u and d masses its behavior in the presence of a magnetic field would be similar to the d quark, essentially dictated by the charge. However, using the current mass of the model, the s quark is much less sensitive to the magnetic field than the light quarks. Due to the 't Hooft term, it has a strong influence on the light quarks at all temperatures for small magnetic fields and

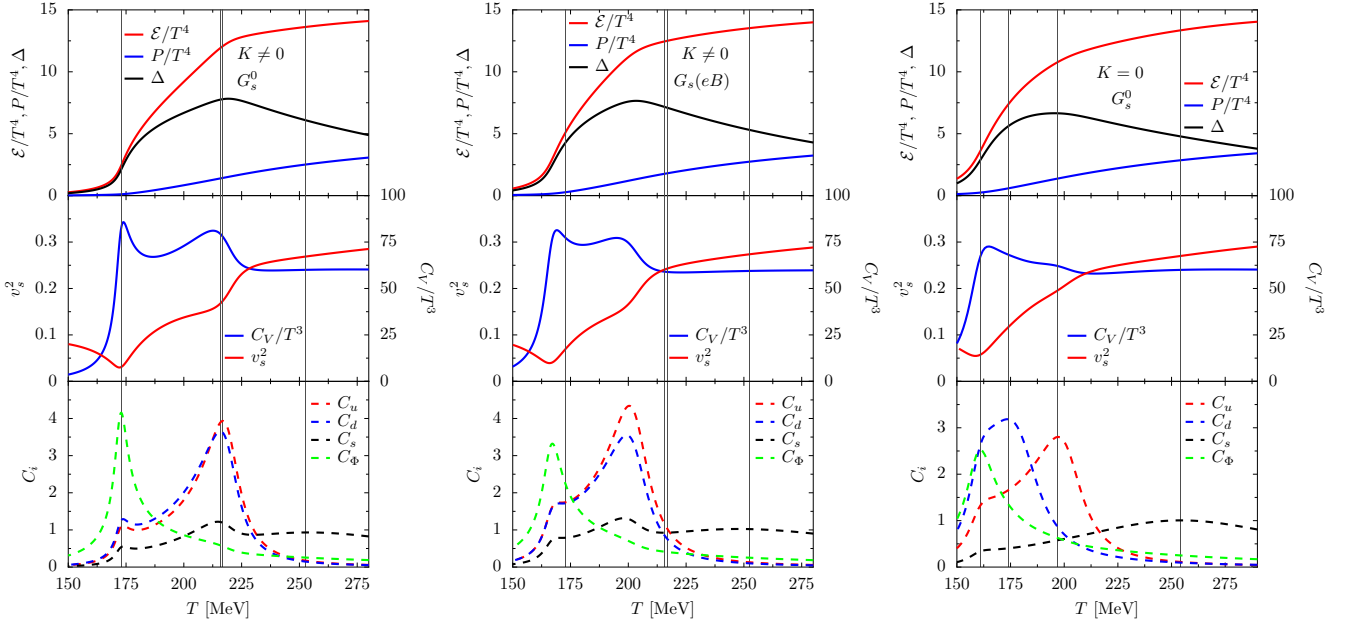


FIG. 12. The scaled energy density \mathcal{E}/T^4 , the interaction measure $\Delta(T) = (\mathcal{E} - 3P)/T^4$, and the scaled pressure P/T^4 as a function of temperature T (top panels); the scaled specific heat C_V/T^3 , and speed of sound squared v_s^2 as a function of temperature T (middle panels); and the quark susceptibilities (bottom panels), for $eB = 0.3 \text{ GeV}^2$ with the 't Hooft term, and $G_s = G_s^0$ (left) or $G_s = G_s(eB)$ (middle) and without the 't Hooft term and $G_s = G_s^0$ (right). The vertical lines in the left and right panels indicate the position of the maximum of the quark susceptibilities. In the middle panel the vertical lines are located at the same temperatures of the left panel.

for temperatures close to the transition temperature and above for strong magnetic fields. In particular, the large mass of the s quark makes the chiral transition of the light sector smoother and shifted to larger temperatures.

It was shown that although with a much weaker effect, the s quark chiral transition temperature is also affected by the magnetic field and increases if a constant scalar coupling is used. However, if the magnetic dependent coupling constant proposed in [39] is considered, the critical temperature associated with the s quark decreases with eB . This effect, known as the inverse magnetic catalysis, is seen on the nonmonotonic behavior of the s quark condensate with the magnetic field.

The 't Hooft term has opposite effects when G_s^0 or $G_s(eB)$ are used: in the first case the s chiral transition is almost not affected by the magnetic field for $0 < eB < 0.45 \text{ GeV}^2$, before being washed out by the transition of the light quarks, while in the second case the pseudocritical temperature has a significant decrease for $0 < eB < 0.55 \text{ GeV}^2$. For a constant coupling the magnetic catalysis increases the u and d quark masses and the transition temperatures, bringing them close to that of the s quark, or above for the u quark and sufficiently strong fields. The flavor mixing induced by the 't Hooft term thus has not much effect on the s quark transition. On the other hand, a coupling $G_s(eB)$ that gets weaker with eB originates the IMC effect close to the transition temperature of the u and d quarks. The s quark will be strongly influenced both directly through the weakening of G_s and by the u and d quarks through

the 't Hooft term, so that its transition temperature will also decrease.

The identification of the s quark chiral transition temperature is only possible below a magnetic field of the order of $eB \sim 0.45 - 0.55 \text{ GeV}^2$, 0.45 GeV^2 for a constant coupling and 0.55 GeV^2 for a field dependent coupling. For larger magnetic fields the s and d quark susceptibilities overlap too strongly.

An important effect of the large mass of the s quark is to push the chiral transition temperatures of the u and d quarks to larger temperatures due to the mixing induced by the 't Hooft term. However, a magnetic field dependent scalar coupling that weakens the interaction for larger magnetic fields has the effect of decreasing both chiral and deconfinement temperatures, more the first ones than the last. In this case a larger overlap between the quark susceptibilities occurs and the signature of the crossover on thermodynamical quantities such as sound velocities or specific heat becomes smoother.

ACKNOWLEDGMENTS: This work was partially supported by Projects PTDC/FIS/113292/2009, PEst-OE/FIS/UI0405/2014 and CERN/FP/123620/2011 developed under the initiative QREN financed by the UE/FEDER through the program COMPETE – “Programa Operacional Factores de Competitividade” and by Grant No. SFRH/BD/51717/2011.

-
- [1] M. Buballa, Phys. Rep. **407**, 205 (2005).
- [2] F. Wilczek, Int. J. Mod. Phys. **A7**, 3911 (1992); K. Rajagopal and F. Wilczek, Nucl. Phys. **B399**, 395 (1993); M. A. Stephanov, K. Rajagopal and E. V. Shuryak, Phys. Rev. Lett. **81**, 4816 (1998).
- [3] N. Glendenning, *Compact Stars*, (Springer, New York, 2000).
- [4] P. B. Demorest *et al.*, Nature (London) **467**, 1081 (2010).
- [5] J. Antoniadis *et al.*, Science **340**, 6131 (2013).
- [6] M. Baldo, G. F. Burgio, and H.-J. Schulze, Phys. Rev. C **61**, 055801 (2000); I. Vidaña, A. Polls, A. Ramos, L. Engvik, and M. Hjorth-Jensen, Phys. Rev. C **62**, 035801 (2000); H.-J. Schulze, A. Polls, A. Ramos, and I. Vidaña, Phys. Rev. C **73**, 058801 (2006).
- [7] I. Vidaña, D. Logoteta, C. Providência, A. Polls, and I. Bombaci, Europhys. Lett. **94**, 11002 (2011).
- [8] R. Cavagnoli, D. P. Menezes, and C. Providência, Phys. Rev. C **84**, 065810 (2011).
- [9] I. Bednarek, P. Haensel, J. L. Zdunik, M. Bejger, and R. Mańka, Astron. Astrophys. **543**, A157 (2012).
- [10] S. Weissenborn, D. Chatterjee, and J. Schaffner-Bielich, Nucl. Phys. **A881**, 62 (2012); S. Weissenborn, D. Chatterjee, and J. Schaffner-Bielich, Phys. Rev. C **85**, 065802 (2012).
- [11] C. Providência and A. Rabhi, Phys. Rev. C **87**, 055801 (2013).
- [12] P. K. Panda, D. P. Menezes, and C. Providência, Phys. Rev. C **89**, 045803 (2014).
- [13] L. Bonanno and A. Sedrakian, Astron. Astrophys. **539**, A16 (2012).
- [14] D. Elia (ALICE Collaboration), J. Phys. Conf. Ser. **455**, 012005 (2013).
- [15] J. Rafelski and B. Muller, Phys. Rev. Lett. **48**, 1066 (1982); [Erratum-ibid. **56**, 2334 (1986)].
- [16] P. Koch, B. Muller, and J. Rafelski, Phys. Rep. **142**, 167 (1986).
- [17] S. Chatterjee, R. M. Godbole, and S. Gupta, Phys. Lett. B **727**, 554 (2013).
- [18] K. A. Bugaev, D. R. Oliinychenko, J. Cleymans, A. I. Ivanytskyi, I. N. Mishustin, E. G. Nikonov and V. V. Sagun, Europhys. Lett. **104**, 22002 (2013).
- [19] A. Bazavov, H. -T. Ding, P. Hegde, O. Kaczmarek, F. Karsch, E. Laermann, Y. Maezawa, S. Mukherjee, *et al.*, arXiv:1404.6511 [hep-lat].
- [20] R. Bellwied, S. Borsanyi, Z. Fodor, S. D. Katz, and C. Ratti, Phys. Rev. Lett. **111**, 202302 (2013).
- [21] Y. Aoki, G. Endrodi, Z. Fodor, S. D. Katz, and K. K. Szabo, Nature (London) **443**, 675 (2006).
- [22] K. Fukushima and C. Sasaki, Prog. Part. Nucl. Phys. **72**, 99 (2013).
- [23] S. Borsanyi *et al.* (Wuppertal-Budapest Collaboration), J. High Energy Phys. **09** (2010) 073.
- [24] A. Bazavov, T. Bhattacharya, M. Cheng, C. DeTar, H. T. Ding, S. Gottlieb, R. Gupta, P. Hegde *et al.*, Phys. Rev. D **85**, 054503 (2012).
- [25] A. Bazavov, H. -T. Ding, P. Hegde, O. Kaczmarek, F. Karsch, E. Laermann, Y. Maezawa, S. Mukherjee *et al.*, Phys. Rev. Lett. **111**, 082301 (2013).
- [26] C. McNeile, A. Bazavov, C. T. H. Davies, R. J. Dowdall, K. Hornbostel, G. P. Lepage and H. D. Trotter, Phys. Rev. D **87**, 034503 (2013).
- [27] K. Fukushima, D. E. Kharzeev, and H. J. Warringa, Phys. Rev. D **78**, 074033 (2008); D. E. Kharzeev and H. J. Warringa, *ibid.* **80**, 034028 (2009); D. E. Kharzeev, Nucl. Phys. **A830**, 543c (2009).
- [28] V. Skokov, A. Y. Illarionov, and V. Toneev, Int. J. Mod. Phys. **A24**, 5925 (2009).
- [29] G. S. Bali, F. Bruckmann, G. Endrodi, Z. Fodor, S. D. Katz, S. Krieg, A. Schafer, and K. K. Szabo, J. High Energy Phys. **02** (2012) 044.
- [30] G. S. Bali, F. Bruckmann, G. Endrodi, Z. Fodor, S. D. Katz, and A. Schafer, Phys. Rev. D **86**, 071502 (2012).
- [31] F. Bruckmann, G. Endrodi, and T. G. Kovacs, J. High Energy Phys. **04** (2013) 112.
- [32] M. Ferreira, P. Costa, D. P. Menezes, C. Providência, and N. Scoccola, Phys. Rev. D **89**, 016002 (2014).
- [33] M. Ferreira, P. Costa, and C. Providência, Phys. Rev. D **89**, 036006 (2014).
- [34] W. -j. Fu, Phys. Rev. D **88**, 014009 (2013).
- [35] P. Costa, M. Ferreira, H. Hansen, D. P. Menezes, and C. Providência, Phys. Rev. D **89**, 056013 (2014).
- [36] R. Gatto and M. Ruggieri, Lect. Notes Phys. **871**, 87 (2013).
- [37] E. S. Fraga, Lect. Notes Phys. **871**, 121 (2013).
- [38] M. D'Elia, Lect. Notes Phys. **871**, 181 (2013).
- [39] M. Ferreira, P. Costa, O. Lourenço, T. Frederico and C. Providência, Phys. Rev. D **89**, 116011 (2014).
- [40] K. Fukushima, Phys. Lett. B **591**, 277 (2004); C. Ratti, M. A. Thaler, and W. Weise, Phys. Rev. D **73**, 014019 (2006).
- [41] T. Hatsuda and T. Kunihiro, Phys. Rep. **247**, 221 (1994); S. P. Klevansky, Rev. Mod. Phys. **64**, 649 (1992).
- [42] D. P. Menezes, M. Benghi Pinto, S. S. Avancini, A. Perez Martinez, and C. Providência, Phys. Rev. C **79**, 035807 (2009); D. P. Menezes, M. Benghi Pinto, S. S. Avancini, and C. Providência, Phys. Rev. C **80**, 065805 (2009).
- [43] P. Rehberg, S. P. Klevansky, and J. Hufner, Phys. Rev. C **53**, 410 (1996).
- [44] S. Roessner, C. Ratti, and W. Weise, Phys. Rev. D **75**, 034007 (2007).
- [45] O. Kaczmarek, F. Karsch, P. Petreczky, and F. Zantow, Phys. Lett. B **543**, 41 (2002).
- [46] Y. Aoki, S. Borsanyi, S. Durr, Z. Fodor, S. D. Katz, S. Krieg, and K. K. Szabo, J. High Energy Phys. **06** (2009) 088.
- [47] K. Fukushima, Phys. Rev. D **77**, 114028 (2008) [Erratum-ibid. D **78**, 039902 (2008)].
- [48] A. J. Mizher, M. N. Chernodub, and E. S. Fraga, Phys. Rev. D **82**, 105016 (2010).
- [49] N. Callebaut and D. Dudal, Phys. Rev. D **87**, 106002 (2013).
- [50] P. Costa, C.A. de Sousa, M. C. Ruivo, and Y. L. Kalinovsky, Phys. Lett. B **647**, 431 (2007); P. Costa, M.C. Ruivo, C.A. de Sousa, and H. Hansen, Symmetry **2**(3), 1338 (2010).
- [51] R. L. S. Farias, K. P. Gomes, G. I. Krein, and M. B. Pinto, arXiv:1404.3931 [hep-ph].
- [52] P. Costa, M. C. Ruivo, C. A. de Sousa, and Yu. L. Kalinovsky, Phys. Rev. D **71**, 116002 (2005).
- [53] S. Borsanyi, Z. Fodor, C. Hoelbling, S. D. Katz, S. Krieg and K. K. Szabo, Phys. Lett. B **730**, 99 (2014).

- [54] G. S. Bali, F. Bruckmann, G. Endrodi, S. D. Katz and A. Schafer, arXiv:1406.0269 [hep-lat].
- [55] G. Endrödi, J. High Energy Phys. **04** (2013) 023.